Nanosecond Relaxation Dynamics of Protein GB1 Identified by the Time-Dependent Red Shift in the Fluorescence of Tryptophan and 5-Fluorotryptophan

Dmitri Toptygin,*,† Angela M. Gronenborn,‡,§ and Ludwig Brand†

Department of Biology, Johns Hopkins University, Baltimore, Maryland 21218, and Laboratory of Chemical Physics, NIDDK, National Institutes of Health, Bethesda, Maryland

Received: July 17, 2006; In Final Form: October 19, 2006

The B1 domain of Streptococcal protein G (GB1) is a small, thermostable protein containing a single tryptophan residue. We recorded time-resolved fluorescence of the wild-type GB1 and its 5-fluorotryptophan (5FTrp) variant at more than 30 emission wavelengths between 300 and 470 nm. The time-resolved emission spectra reveal no signs of heterogeneity, but show a time-dependent red shift characteristic of microscopic dielectric relaxation. This is true for both 5FTrp and unmodified Trp in GB1. The time-dependent red shifts in the fluorescence of 5FTrp and unmodified Trp are essentially identical, confirming that the shift is caused by the relaxation of the protein matrix rather than by the fluorophore itself. The total amplitude (but not the rate) of the time-dependent red shift depends on the fluorophore, specifically, on the magnitude of the vector difference between its excited state and ground state electric dipole moments; for 5FTrp this is estimated to be about 88% of that for the unmodified Trp. The decay of the excited state fluorophore population is not monoexponential for either fluorophore; however, the deviation from the monoexponential decay law is larger in the case of unmodified Trp. The relaxation dynamics of GB1 was found to be considerably faster than that of other proteins studied previously, consistent with the small size, tightly packed core, and high thermodynamic stability of GB1.

Introduction

The time-dependent red shift[1] in the fluorescence of solvatochromic dyes has been widely used to study solvent relaxation dynamics of polar solvents.[2−5] It has also been employed to study the relaxation dynamics of proteins,[6−18] membranes,[19] and DNA.[20] The fundamental origin of the shift is in the difference between the π-electron density distributions corresponding to the ground and excited state of a fluorescent molecule. For a solvatochromic fluorophore this difference is particularly large, therefore, exciting such a fluorophore produces a significant charge shift. The charge shift gives rise to a relaxation process, during which nearby charged and polar groups readjust their positions and orientations. This motion of charges generates a time-variant reaction field that acts back on the fluorophore and modulates the energy gap between its ground and excited state (linear Stark effect). The time variation of the energy gap reveals itself in the form of the time-dependent red shift that reflects the dynamics of microscopic dielectric relaxation in the fluorophore environment, whether this environment is a polar solvent or a protein matrix.

One general consequence of the time-dependent red shift is that the kinetics of the fluorescence emission intensity after a short excitation pulse is not monoexponential[21] and different in different parts of the emission spectrum. If the characteristic relaxation time is much shorter than the excited state lifetime, then deviations of the fluorescence intensity from the monoexponential behavior last only a few characteristic relaxation times after the excitation pulse, and the remaining part of the fluorescence kinetic curve is monoexponential. The characteristic relaxation times of low-viscosity polar solvents, such as water,[3] acetonitrile,[4,5] and tetrahydrofuran,[4,5] are of the order of 1 ps, therefore the fluorescence kinetics of solvatochromic dyes in these solvents are monoexponential except for the first 10 ps after the excitation pulse. If a time-correlated single-photon-counting (TCSPC) instrument with a typical time resolution of the order of 100 ps is used to record the emission, then the recorded kinetics appear to be perfectly monoexponential. Relaxation of a high-viscosity polar solvent, such as anhydrous glycerol, can take several nanoseconds; in this case TCSPC kinetic curves vary with the emission wavelength and cannot be fit by the monoexponential model function.[22]

It was long recognized that the spectrum of normal vibrations of a protein macromolecule contains very low frequencies[23] not found in vibrational spectra of small molecules. The low-frequency normal vibrations are damped by the viscous drag of the solvent,[23] which transforms their impulse response dynamics from sinusoidal oscillations to aperiodic relaxation. For a protein macromolecule of several kD molecular weight the lowest vibrational frequencies are usually under 1 GHz, corresponding to relaxation times longer than 1 ns. Thus, even if an instrument with a time resolution of the order of 100 ps is used, the time-resolved fluorescence of a solvatochromic fluorophore in a protein matrix is not expected to be monoexponential. This is in agreement with experimental data obtained by using several solvatochromic fluorophores, including 2,6-*p*-TNS,[6−8] DANCA,[9] acrylodan,[10] 2,8-ANS,[11] tryptophan,[14,15] bis-ANS,[17] and porphyrin.[18] More than one exponential is required to describe the time-resolved fluorescence of these fluorophores measured by TCSPC instruments[6,7,9,14,15,17,18] or

* Address correspondence to this author. E-mail: toptygin@jhu.edu.
† Johns Hopkins University.
‡ National Institutes of Health.
§ Current address: Department of Structural Biology, University of Pittsburgh School of Medicine, Pittsburgh, PA.

10.1021/jp064528n CCC: $33.50
Published on Web 12/07/2006

by frequency-domain instruments,[8,10,11] which, in terms of their time resolution, are roughly comparable to TCSPC instruments.

Femtosecond protein dynamics is usually measured by using transient hole burning,[12] photon echo spectroscopy,[13] and fluorescence upconversion.[16] Only the latter method records a fluorescence signal. The upconverted fluorescence emission of aladan, a synthetic fluorescent amino acid incorporated in a protein polypeptide chain,[16] is clearly not monoexponential during the first 50 ps, a time window inaccessible for TCSPC and frequency-domain instruments. Summarizing the results of all experimental studies quoted here, we conclude that the fluorescence of solvatochromic dyes in protein macromolecules is usually found to be monoexponential neither on the picosecond nor on the nanosecond time scale.

A recently published experimental study[24] reported that the time-resolved fluorescence of 5-fluorotryptophan (5FTrp) in single-5FTrp-containing mutants of the mannitol permease (EII^{mtl}) is monoexponential, unlike that of the solvatochromic fluorophores mentioned above. This finding can have several possible explanations. It is possible that 5FTrp is not solvatochromic (or significantly less solvatochromic than the normal Trp); however, this possibility has been ruled out in a recent study of the effect of solvent polarity on the steady state fluorescence spectra of 5FTrp.[25] It is also possible that in the EII^{mtl} mutants the environment of the fluorophores is completely nonpolar. It is also possible that the time-resolved fluorescence of 5FTrp is monoexponential (or nearly monoexponential) at one emission wavelength near the center of the emission spectrum, but multiexponential[21] at the emission wavelengths far from the center (this situation is typical for most solvatochromic fluorophores under the conditions where the amplitude of the red shift is small as compared to the width of the emission spectrum). It is also possible that the relaxation dynamics of the EII^{mtl} matrix is faster than the time resolution of the instrument used in ref 24. At present it is not clear which of the explanations is responsible for the apparent monoexponential fluorescence behavior of 5FTrp in the EII^{mtl} mutants. However, from our viewpoint, a more interesting question is whether the time-dependent red shift can be observed in the fluorescence of 5FTrp in the matrix of any protein at all. This is the first question we attempted to address in the present study.

For our investigation of 5FTrp fluorescence we selected the B1 immunoglobulin-binding domain of streptococcal protein G (GB1). This protein was chosen based on four major considerations. First, the wild-type GB1 protein contains a single Trp residue, which is readily replaced by 5FTrp. Second, GB1 is a well-studied protein; its NMR[26,27] and X-ray crystal[28] structures are available. Third, the high thermal stability of GB1 (reversible melting at 87 °C)[26] precludes the presence (at lower temperatures) of partially folded and fluctuating conformations that naturally may give rise to heterogeneity in the fluorescence signal. Fourth, the dielectric relaxation of the GB1 matrix has been successfully measured using aladan, a synthetic fluorescent amino acid incorporated in GB1 at the location of the Trp residue.[16]

As we stated earlier, the first question we attempted to address is whether the time-dependent red shift can be observed in the fluorescence of 5FTrp in the GB1 matrix. To answer this question, we have measured spectrally and time-resolved fluorescence of 5FTrp in GB1—this type of measurement has never been done with 5FTrp in any protein. The second question we attempted to address is whether the kinetics of the time-dependent red shift in the fluorescence of 5FTrp is the same as that in the fluorescence of unmodified Trp. If the time-dependent red shift reflects the dynamics of microscopic dielectric relaxation in the GB1 matrix, then the kinetics of the time-dependent red shifts should be similar for 5FTrp and unmodified Trp. If the time-dependent red shift is due to an internal mechanism, then it is expected that the kinetics should be dissimilar for the two fluorophores.

The third question we attempted to address is related to the decay of the excited state 5FTrp population in the GB1 matrix. In the absence of the time-dependent spectral shift, the kinetics of fluorescence emission intensity is the same in every part of the emission spectrum and represents the decay of the excited state population. In the presence of the time-dependent spectral shift, the kinetics of fluorescence emission intensity is different in different parts of the emission spectrum; the decay of the excited state population can be reconstructed by integrating appropriately weighted fluorescence kinetic curves over the emission spectrum (vide infra). It is not of great importance whether the decay of the excited state 5FTrp population is monoexponential or not, because the answer to this absolute question depends on the quality of the data and on the statistical criteria employed to detect deviations of the data from a monoexponential kinetic curve. Thus, what one researcher calls monoexponential can be multiexponential[21] from the point of view of another researcher. The answer to the relative question, whether the deviation from the monoexponential decay law is greater for unmodified Trp than for 5FTrp, should be independent of the data quality (as long as the data of comparable quality are used for both fluorophores) and of the statistical criteria. This relative question is the third question that we attempted to address in the present study.

Experimental Section

Protein Expression and Purification. Both 5FTrp-substituted and unsubstituted wild-type GB1 protein were expressed in *E. coli* BL-21 (DE3), using the pET11a vector system. To produce the 5FTrp GB1 variant, cultures were grown at 37 °C, using excess 5FTrp as the sole source of tryptophan in a defined, modified minimal medium. Cells were harvested 3−4 h after induction and frozen at −80 °C. Frozen cells were thawed by suspending them in PBS buffer (1 g cells/ 5 mL buffer) at 0 °C. The cell suspension was heat treated at 80 °C for 5 min and immediately chilled on ice for 10 min. Precipitated denatured proteins as well as cell debris were removed by centrifugation in an SS34 rotor at 14 000 rpm. The supernatant contained predominantly GB1, which was purified further by reversed-phase HPLC on POROS 20 R2 resin (PreSeptive Biosystems, Framingham, MA), using a linear water/acetonitrile gradient. The identity and final purity of the proteins were verified by mass spectrometry and SDS-PAGE. The percentage labeling was established by NMR and mass spectrometry and was found to be >95%. The 5FTrp-substituted wild-type GB1 exhibited a molecular mass of 6241 g/mol, closely matching the expected mass of 6237 g/mol. Analysis of spectrally and time-resolved fluorescence data confirmed >97% labeling (at ≤97% labeling the analysis would reveal heterogeneity). For storage, the protein was dialyzed into water or 50 mM sodium phosphate buffer, pH 5.5, and kept at 4 °C.

Fluorescence Measurements. For fluorescence measurements each protein was diluted to 60 μM concentration and dialyzed against a 20 mM sodium phosphate buffer containing 0.02% NaN_3, pH 6.0. All fluorescence measurements were carried out at +5 °C. Time-correlated single-photon counting (TCSPC) data were obtained with a home-built instrument; its schematic diagram is provided in the Supporting Information.

Fluorescence was excited by a frequency-doubled output from a cavity-dumped dye laser. The exciting radiation was a train of 11 ps wide pulses with a repetition rate of 4.1 MHz. To avoid contaminating the fluorescence signal by the emission from photobleached Trp,[29] the exciting power was attenuated to 2 μW or less and the exciting beam was defocused so that the power density did not exceed 1 μW/mm^2. Fluorescence emission passed through a polarizer and a monochromator (H10, Jobin Yvon) and was detected by a microchannel plate photomultiplier (R1564U, Hamamatsu). To avoid pile-up errors, anode current pulses were counted at a rate not exceeding 20 kHz and stored in 2048 channels, with the timing calibration of 13.33 ps/channel. Impulse response function (IRF) was recorded with a Ludox scatterer cell and had a full width of 65 ps at half-maximum (see Figures 2S and 3S in the Supporting Information); this represents the time resolution of the entire system. The IRF was found to slowly drift with time; during 8 h of continuous measurements the peak could drift by as much as 25 ps on the time scale. To cancel the systematic errors that could result from this drift, a corresponding IRF was recorded quasisimultaneously with every fluorescence kinetic curve; out of every 1 min the instrument dwelled on the scatterer cell for about 10 s and on the fluorescence cell for about 50 s; the IRF and the fluorescence kinetic curve were stored in different 2K memory segments of the multichannel analyzer (ADCAM 918, EG&G Ortec); computer-controlled motors quickly swapped the cells and moved the emission monochromator between the exciting and emission wavelength. Steady state fluorescence emission spectra were measured on an SLM-48000 spectrofluorometer (SLM Instruments, Urbana, Illinois) and corrected for both the spectral variation of the emission channel sensitivity and the inner-filter effect as described earlier.[15] To minimize the excitation of tyrosine residues, a 296 nm exciting wavelength was used for both steady state and time-resolved measurements; the bandwidth of the exciting radiation was 2 nm in the case of steady state measurements and much less than that in the case of time-resolved measurements. The bandwidth of the emission monochromators was 8 nm in all cases. The emission monochromators were scanned from 300 to 450 nm (unmodified Trp) or from 305 to 470 nm (5FTrp); the wavelength increment was 1 nm in the steady state spectra and 5 nm between TCSPC kinetic curves. All fluorescence measurements were carried out under the magic angle polarizer configuration. For steady state measurements the polarizer in the excitation channel was set to 55° from vertical and the one in the emission channel was set to vertical to avoid Wood's anomalies in the emission spectra. For time-resolved measurements the exciting radiation was vertically polarized, and the polarizer in the emission channel was set to 55° from vertical.

Data Analysis. Each experimental TCSPC kinetic curve was fitted by a numerical convolution of the quasisimultaneously acquired IRF with the following model function

$$F_m(t) = b_m + s_m\delta(t) + \theta(t)\sum_{n=1}^{N_{\exp}}\alpha_{mn}\exp(-t/\tau_n) \qquad (1)$$

The index m is relevant to the global analysis only, representing the serial number of the wavelength at which the emission was collected; $\delta(t)$ and $\theta(t)$ are Dirac delta and Heaviside step functions, respectively; $N_{\exp}$ denotes the total number of exponentials; the free fitting parameters b_m, s_m, α_{mn}, and τ_n are the photomultiplier background (dark counts), the intensity of scattered exciting radiation (including Raman), the pre-exponential amplitudes (allowed to be both positive and negative), and the time constants. The fitting procedure used a nonlinear weighted least-square algorithm to minimize χ^2. The weights were calculated by using the a priori knowledge that fluorescence photons are emitted independently of one another and therefore photon counts must follow Poissonian statistics. The quality of the fits was judged by the reduced χ^2 values, by plots of weighted residuals, and by the autocorrelation plots; these plots generated by the single-curve analysis program TCPHOTON are provided in the Supporting Information.

We previously showed that for multiexponential time-resolved fluorescence being caused by the time-dependent red shift, the time constants τ_n must have the same values at every emission wavelength.[15,22] If multiexponential time-resolved fluorescence is due to static heterogeneity, then the time constants τ_n represent the lifetimes of different fluorophores (or one fluorophore in different states or different environments), and in this case the τ_n values are also expected to be wavelength invariant.[30] Thus, regardless of the origin of the multiexponentiality, one should fit the data by a model that keeps the fitting parameters τ_n the same for all kinetic curves; the kinetic curves obtained at different emission wavelengths must be fit simultaneously in this case. Global (simultaneous) fitting of up to 34 kinetic curves obtained at different emission wavelengths was done using the program L_GLOBAL described previously.[31] After the global fitting, the values of the pre-exponential amplitudes α_{mn} were renormalized so that for every m, the sum of the products $\alpha_{mn}\tau_n$ over all n would be equal to the corrected steady state emission intensity at the corresponding emission wavelength λ_m. This renormalization eliminated any systematic errors associated with the spectral variation of the emission channel sensitivity, the instability of the exciting power, and the dead time of some electronic modules involved in TCSPC. Technical details of the renormalization, spectral correction, polynomial smoothing of the pre-exponential amplitude spectra, and conversion from wavelength to wavenumber scale have been described elsewhere.[15]

Characterization of the Time-Dependent Red Shift. The dynamics of the time-dependent red shift is commonly studied by looking at the time variation of the peak or the center of gravity of the emission spectrum. The center of gravity is less affected by the random noise in the data. For a spectrum expressed as a function of wavelength (λ), the center of gravity is not linearly related to the energy gap between the ground and excited electronic states. In contrast, for a spectrum expressed as a function of wavenumber (ν) and multiplied by ν^{-3} (to compensate for the general ν^3 dependence of the rate of electric dipole emission), the center of gravity equals the electronic energy gap plus a constant.[22] In the following, the center of gravity of the product $\nu^{-3}F_\nu$ is denoted $\bar{\nu}$ and is strictly defined as follows:

$$\bar{\nu}(t) = \frac{\int_0^\infty \nu[\nu^{-3}F_\nu(\nu,t)]\,d\nu}{\int_0^\infty [\nu^{-3}F_\nu(\nu,t)]\,d\nu} \qquad (2)$$

Here F_ν represents the emitted photon density per unit wavenumber per unit time. At $t > 0$ the spectrally and time-resolved intensity $F_\nu(\nu,t)$ can be approximated by a sum of exponentials:

$$F_\nu(\nu,t) = \sum_{n=1}^{N_{\exp}}\alpha_n(\nu)\exp(-t/\tau_n) \qquad (3)$$

Substituting $F_\nu(\nu,t)$ from eq 3 into eq 2 and taking the sums out from under the integral signs yields the following convenient

expression for calculating $\bar{\nu}(t)$:

$$\bar{\nu}(t) = \frac{\sum_{n=1}^{N_{exp}} J_n^{\,2} \exp(-t/\tau_n)}{\sum_{n=1}^{N_{exp}} J_n^{\,3} \exp(-t/\tau_n)} \tag{4}$$

where J_n^2 and J_n^3 are two of the family of time-invariant spectral moments

$$J_n^{\,p} = \int_0^{\infty} \nu^{-p} \alpha_n(\nu)\, d\nu \tag{5}$$

If the data were collected on a set of equally spaced wavelengths λ_m that cover the entire emission spectrum, then the spectral moments can be directly calculated from the values of the fitting parameters α_{mn} and τ_n, which are determined in the course of the global analysis:

$$J_n^{\,p} = \sum_m \lambda_m^{\,p} \alpha_{mn} \frac{F_{ss}(\lambda_m)}{\sum_i \alpha_{mi}\tau_i} \tag{6}$$

In eq 6 $F_{ss}(\lambda)$ is the corrected steady state emission spectrum; renormalization of α_{mn} using the steady state intensity takes care of the laser intensity variations, dead time, etc.

For some representations of the dynamic spectral shift it is necessary to evaluate the $t \rightarrow \infty$ limit of $\bar{\nu}(t)$, which is denoted $\bar{\nu}(\infty)$. From eq 4 it directly follows that

$$\bar{\nu}(\infty) = \frac{J_l^{\,2}}{J_l^{\,3}} \tag{7}$$

where l corresponds to the exponential with the longest τ, i.e., τ_l is the longest of all τ_n.

Characterization of the Excited State Population Decay. The variation of the number N of fluorescent molecules in the excited state with the time t after excitation describes the decay of the excited state population, $N(t)$. In the absence of the time-dependent red shift, the time-resolved fluorescence emission in any part of the emission spectrum equals $N(t)$ times a constant factor, therefore any fluorescence kinetic curve also can be called a decay curve. This is not the case in the presence of the time-dependent red shift. As we have shown earlier,[22,15] the spectrally and time-resolved intensity $F_\nu(\nu,t)$ has the following relation to the decay law $N(t)$:

$$F_\nu(\nu,t) = a\nu^3 S[\nu - \bar{\nu}(t)]|\mu_{01}(t)|^2 N(t) \tag{8}$$

In eq 8 a is a constant scale factor; $S(x)$ represents the Franck−Condon factor envelope; $\bar{\nu}(t)$ is defined in eq 2; and $|\mu_{01}(t)|^2$ is the squared magnitude of the electric dipole moment responsible for the radiative transitions between the singlet electronic energy levels 1 (excited) and 0 (ground).

Multiplying both sides of eq 8 by ν^{-3} and integrating the products by $d\nu$ over the entire emission spectrum yields

$$\int_0^{+\infty} \nu^{-3} F_\nu(\nu,t)\, d\nu = a|\mu_{01}(t)|^2 N(t) \int_0^{+\infty} S[\nu - \bar{\nu}(t)]\, d\nu \tag{9}$$

By definition,[22] the function $S(x)$ satisfies the normalization condition

$$\int_{-\infty}^{+\infty} S(x)\, dx = 1 \tag{10}$$

Condition 10 is a direct consequence of the well-known fact that the sum of the Franck−Condon factors over all vibrational states equals unity. From the normalization condition it follows that the integral on the right-hand side of eq 9 equals unity, yielding

$$\int_0^{+\infty} \nu^{-3} F_\nu(\nu,t)\, d\nu = a|\mu_{01}(t)|^2 N(t) \tag{11}$$

A further simplification can be achieved by taking time derivatives of the natural logarithms of both sides of eq 11:

$$\frac{\partial}{\partial t} \ln\left[\int_0^{+\infty} \nu^{-3} F_\nu(\nu,t)\, d\nu\right] = \frac{\partial \ln|\mu_{01}(t)|^2}{\partial t} + \frac{\partial \ln[N(t)]}{\partial t} \tag{12}$$

The external electric field that modulates the energy gap between the excited and ground electronic states of the fluorophore also affects the magnitude of the transition moment μ_{01}. An analytical expression describing $|\mu_{01}|^2$ dependence on the external electric field can be found in ref 22. According to our estimates, the time variation of $|\mu_{01}|^2$ during microscopic dielectric relaxation on the picosecond and nanosecond time scales is insignificant, and therefore the first term on the right-hand side of eq 12 is close to zero. Omitting this term and swapping the right- and left-hand sides of eq 12 yields

$$\frac{\partial \ln[N(t)]}{\partial t} = \frac{\partial}{\partial t} \ln\left[\int_0^{+\infty} \nu^{-3} F_\nu(\nu,t)\, d\nu\right] \tag{13}$$

If the spectrally and time-resolved intensity $F_\nu(\nu,t)$ is represented by the sum of exponentials in eq 3, then at $t > 0$

$$\int_0^{+\infty} \nu^{-3} F_\nu(\nu,t)\, d\nu = \sum_{n=1}^{N_{exp}} J_n^{\,3} \exp(-t/\tau_n) \tag{14}$$

where J_n^3 symbols denote the time-invariant spectral moments defined in eq 5, which can be calculated directly from the values of the fitting parameters α_{mn} and τ_n by using eq 6.

It is not difficult to take a time derivative of the natural logarithm of the right-hand side of eq 14 and substitute the result for the right-hand side of eq 13:

$$-\frac{\partial \ln[N(t)]}{\partial t} = \frac{\sum_{n=1}^{N_{exp}} J_n^{\,3} \tau_n^{-1} \exp(-t/\tau_n)}{\sum_{n=1}^{N_{exp}} J_n^{\,3} \exp(-t/\tau_n)} \tag{15}$$

Equation 15 gives a simple practical way of calculating a time derivative of the logarithm of the decay law $N(t)$ for $t > 0$. Note that in the case of a monoexponential decay $-\partial \ln[N(t)]/\partial t$ is constant at $t > 0$ and equals the inverse of the excited state lifetime. Thus, in terms of distinguishing between a monoexponential and a non-monoexponential excited state population decay, being able to calculate $-\partial \ln[N(t)]/\partial t$ is even better than being able to calculate $N(t)$. Any deviation of $-\partial \ln[N(t)]/\partial t$ from a constant indicates a deviation of the excited state population decay from a monoexponential decay law. Furthermore, the greater the range of variation of $-\partial \ln[N(t)]/$

TABLE 1: Reduced χ^2 Values for Single-Curve Fits to Fluorescence Emission of 5FTrp and Unmodified Trp in GB1 at Selected Emission Wavelengths[a]

	5FTrp			unmodified Trp		
N_{exp}	325 nm	355 nm	390 nm	320 nm	350 nm	385 nm
1	11.460	3.588	2.684	29.752	11.583	5.681
2	2.619	0.983	1.726	4.618	1.049	3.982
3	1.093	0.982	1.031	1.155	1.041	1.072
4	1.003	0.977	0.992	0.968	1.036	1.003
5	1.002	0.978	0.993	0.968	1.035	1.003

[a] The underlined values correspond to the smallest N_{exp} sufficient for an adequate fit.

∂t, the more non-monoexponential is the decay of the excited state population.

Results and Discussion

Single-Curve Fits. Fluorescence kinetic curves were collected at more than 30 different emission wavelengths. The kinetic curves were first fitted one at a time (single-curve fitting) by the model based on eq 1 with $N_{exp} = 1$, 2, 3, 4, and 5. The reduced χ^2 values for six representative kinetic curves are shown in Table 1. For an adequate fit to the data with about 2000 degrees of freedom,[32] with a probability of 99% the reduced χ^2 value should lie between 0.919 and 1.081; a reduced χ^2 outside this range indicates that the model function is inadequate.[33] According to this test, the monoexponential model function ($N_{exp} = 1$) produced inadequate fits to all kinetic curves, both for 5FTrp and for unmodified Trp. On the other hand, multiexponential model functions ($N_{exp} > 1$) with varying numbers of exponential terms (N_{exp}) produced adequate fits to all kinetic curves. In Table 1 we have underlined the reduced χ^2 values corresponding to the smallest N_{exp} that was sufficient for a statistically adequate fit to a specific kinetic curve (the values of the best-fit model parameters α_n and τ_n for these N_{exp} can be found in the Supporting Information). For each fluorophore there is only one emission wavelength at which the double-exponential ($N_{exp} = 2$) fit was adequate; this wavelength (355 nm for 5FTrp and 350 nm for unmodified Trp) is close to the center of the emission spectrum of the fluorophore. At any other emission wavelength, whether it is included in Table 1 or not, three or four exponential terms were required for a statistically adequate single-curve fit.

A graphical comparison of single-curve fits to one representative kinetic curve is presented in Figure 1. Autocorrelation plots (displayed at the top of Figure 1) are extremely sensitive to small systematic errors, and, in our opinion, offer the best way for discriminating between adequate and inadequate fits, even better than the reduced χ^2 test. In the Supporting Information we provide plots of the data with fits, weighted residuals, and autocorrelation of the residuals for six selected emission wavelengths (325, 355, and 390 nm for 5FTrp and 320, 350, and 385 nm for unmodified Trp) and for five model functions ($N_{exp} = 1$, 2, 3, 4, and 5); a total of 30 figures.

The autocorrelation plots and the reduced χ^2 test clearly show that the time-resolved emission of 5FTrp in GB1 is not monoexponential, in contrast to previous reports on 5FTrp fluorescence in several single-5FTrp-containing mutants of the mannitol permease[24] and α-synuclein.[34] It should be emphasized that this difference is primarily due to the difference in the quality of data and in the usage of rigorous statistical criteria. In this work fluorescence kinetics was measured at 34 different emission wavelengths and the peak photon counts in the kinetic curves measured near the peak emission wavelength are close

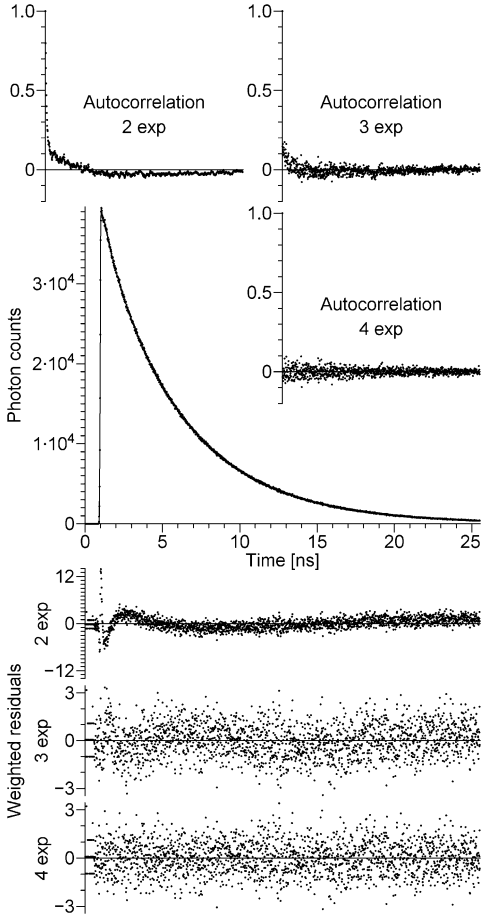

Figure 1. Time-resolved fluorescence of 5FTrp GB1 at 325 nm emission wavelength, fitted by model functions with $N_{exp} = 2$, 3, and 4. Experimental data (points) and the quadruple-exponential fit (continuous line) are shown in the panel labeled "Photon counts"; in this representation it is impossible to detect systematic errors associated with an inadequate fit. Systematic errors associated with the double- and triple-exponential fits are clearly discernible in the plots of weighted residuals (bottom panel). Autocorrelation of unweighted residuals (top panel plots) provides the best representation for the detection of small systematic errors.

to 80×10^3, whereas in refs 24 and 34 fluorescence kinetics was measured at one emission wavelength and the peak photon counts are close to 7×10^3 in ref 24 (in ref 34 the peak counts are not specified). For a fair comparison between our data and the data from ref 24 we took a few fluorescence kinetic curves with only 7×10^3 peak counts and presented them in the format of Figure 1 from ref 24; our data presented in this manner can be found in Figure 34S in the Supporting Information. Upon a visual inspection the kinetic curves in Figure 34S appear to be monoexponential; furthermore, this is true not only for 5FTrp, but also for unmodified Trp in the GB1 matrix. This clearly demonstrates that on a semilogarithmic plot like those in Figure 34S or in refs 24 and 34 it is virtually impossible to detect the minute difference between a monoexponential and a multiexponential kinetic curve.[35] In the semilogarithmic representation too little weight is placed on the data in the beginning of the kinetic curve and too much at its tail, where the information content is minimal due to the small signal-to-noise ratio.[35]

The quality of monoexponential fits to the reduced-photon-count kinetic curves also can be judged by using reduced χ^2 values, which are included in Figure 34S in the Supporting Information and in Figure 1 in ref 24 (no reduced χ^2 values are reported in ref 34). In the case of our 5FTrp data the reduced χ^2 does not exceed 1.19, which is not higher than most of the

TABLE 2: Reduced χ^2 Values for Global Fits to Fluorescence Emission of 5FTrp and Unmodified Trp in GB1 at All Emission Wavelengths[a].

	$N_{exp} = 1$	$N_{exp} = 2$	$N_{exp} = 3$	$N_{exp} = 4$	$N_{exp} = 5$	$N_{exp} = 6$
5FTrp	2.353	1.369	1.037	1.002	1.001	1.001
Trp	4.956	2.134	1.075	1.004	1.003	1.003

[a] The fitting function is based on eq 1.

reduced χ^2 values reported in Figure 1 in ref 24, but is significantly higher than what the χ^2 test[33] tolerates for an adequate fit to the data with 2000 or more degrees of freedom.[32] Thus, according to the rigorous statistical test, even at 7×10^3 peak counts 5FTrp fluorescence is not monoexponential. The similar χ^2 values show that the fluorescence kinetics of 5FTrp in GB1 is not fundamentally different than that of 5FTrp in the mannitol permease.[24] Using higher quality data and rigorous statistical criteria we have shown that the fluorescence kinetics of 5FTrp in GB1 is not monoexponential at any emission wavelength investigated. The same holds true for unmodified Trp in GB1.

Global Fits. Global fitting of 5FTrp GB1 data involved 34 kinetic curves measured at different emission wavelengths (31 kinetic curves in the case of unsubstituted GB1); this corresponds to a little more than 60 000 degrees of freedom.[32] For an adequate fit to the data with 60 000 degrees of freedom, with a probability of 99% the reduced χ^2 value should lie between 0.985 and 1.015; a reduced χ^2 outside this range indicates that the model function is inadequate.[33] Reduced χ^2 values for the global fits by the models involving different numbers of exponential terms are summarized in Table 2. Four exponential terms are necessary for a statistically adequate fit, both in the case of 5FTrp and in the case of unsubstituted Trp in GB1.

The pre-exponential amplitudes α_{mn} and time constants τ_n that minimized the global χ^2 in the case of the quadruple-exponential model function are depicted in Figure 2 in the form of pre-exponential factor spectra on a linear wavenumber scale; the corresponding time constants τ_n are listed next to the individual curves. Two of the four pre-exponential factor spectra cross zero at nearly identical abscissae, corresponding to the emission wavelength of about 355 nm in the case of 5FTrp and 350 nm in the case of the unmodified Trp; this fact explains why the double-exponential model gave adequate single-curve fits to the data recorded at these emission wavelengths.

For the unmodified Trp in GB1 decay-associated spectra (DAS) similar to those shown in Figure 2 were published previously.[36] Minor differences between the spectra shown here and those previously published exist. The DAS shown in ref 36 represent the products $\tau_n\alpha_n(\lambda)$ plotted on a linear wavelength scale, whereas in Figure 2 we plotted the pre-exponential factors $\alpha_n(\nu)$ on a linear wavenumber scale. The longest time constant τ_n measured here (7.15 ns) is longer than that reported in ref 36 (5.90 ns); this can be explained by differences in experimental conditions: the lower temperature (+5 °C in this work versus +20 °C in ref 36) and the less acidic buffer (pH 6.0 in this work versus pH 5.7 in ref 36) decrease the nonradiative decay rate and therefore result in an increased lifetime of the excited state. We also note a difference in the full width at half-maximum of the impulse response function: about 65 ps in this work versus 650 ps in ref 36, the limited time resolution of the experimental setup used in the previous study did not allow the resolution of the exponential terms with $\tau_1 = 73$ ps, $\tau_2 = 580$ ps, and $\tau_3 = 3.09$ ns; these unresolved terms were approximated by one exponential with a τ in the range from 440 ps to 2.1 ns. Aside from these differences in the presentation

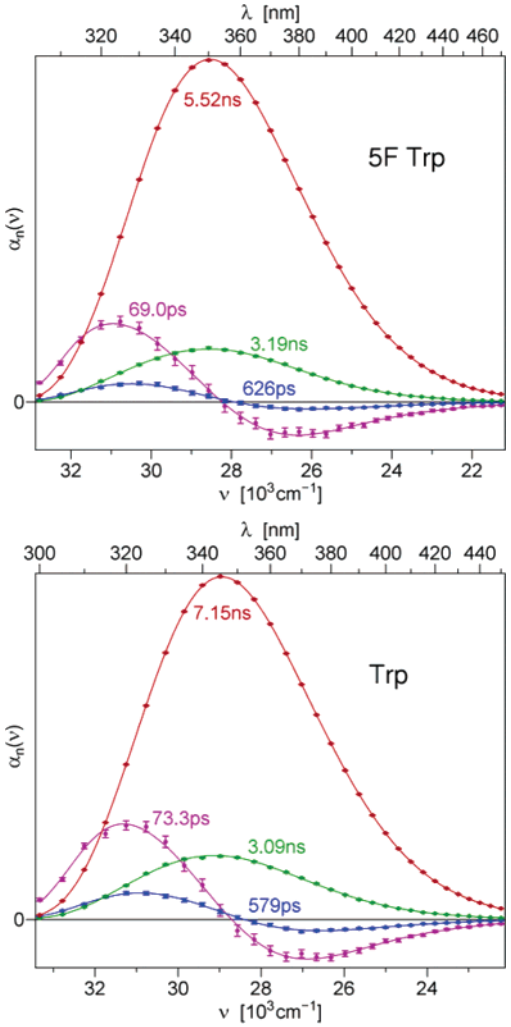

Figure 2. The model parameters resulting in the best global fit to the fluorescence emission of 5FTrp (top panel) and unmodified Trp (bottom panel) in GB1. The model function is based on eq 1 with $N_{exp} = 4$. Dots represent the pre-exponential amplitudes α_{mn}; error bars represent 95% confidence intervals for the amplitudes; smooth curves were produced as described earlier.[15] The corresponding time constant τ_n is printed near each curve, using a matching color.

format and experimental conditions, no other substantial differences between the previously published DAS of the wild-type GB1 and the spectra shown in the bottom panel of Figure 2 exist. No decay-associated spectra or pre-exponential factor spectra of 5FTrp in any protein have been published prior to our current work.

Spectral Dynamics. Two of the four pre-exponential factors are negative on the red side of the zero-crossing point; the negative amplitudes may indicate the presence of an excited state reaction or a relaxation process: in both cases a fluorophore with the red-shifted emission does not exist at the time of excitation, but it is formed later, either as a product of a chemical reaction or as a result of rotation of polar groups (or translation of charged groups) in the vicinity of a solvatochromic fluorophore.

One possible way of distinguishing between an excited state chemical reaction with a small number of states (e.g., a two-state or three-state reaction) and a continuous dielectric relaxation process with an infinite number of intermediate states requires the investigation of the time variation of the instantaneous emission spectrum: in the case of continuous dielectric relaxation, the width of this spectrum is not expected to vary

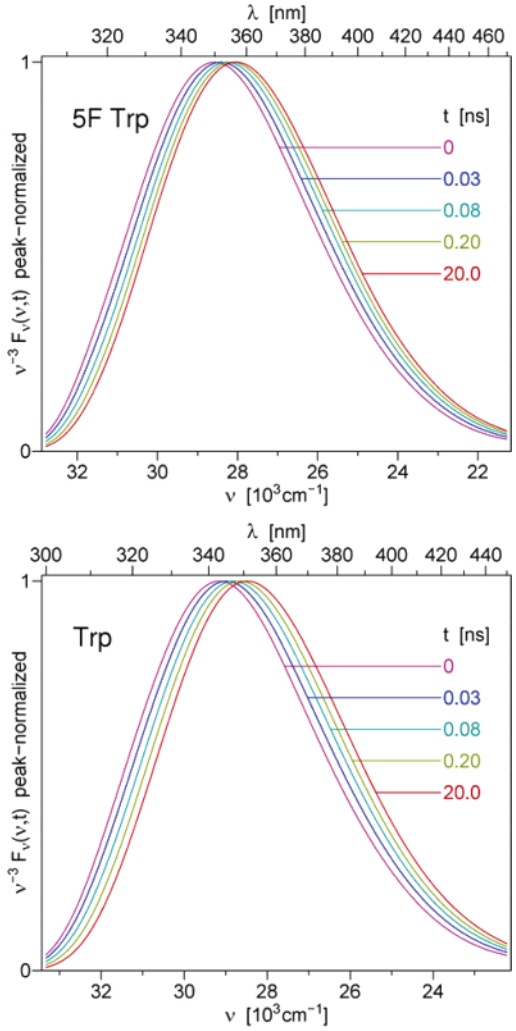

Figure 3. Instantaneous spectra of fluorescence emission from 5FTrp (top panel) and unmodified Trp (bottom panel) in GB1, generated by substituting the pre-exponential factor spectra $\alpha_n(\nu)$ shown in Figure 2 by smooth curves and the values of the time constants τ_n in the equation $F_\nu(\nu,t) = \sum\alpha_n(\nu)\exp(-t/\tau_n)$. The spectra were generated for five different values of t (shown near each curve), multiplied by ν^{-3}, and peak-normalized prior to plotting.

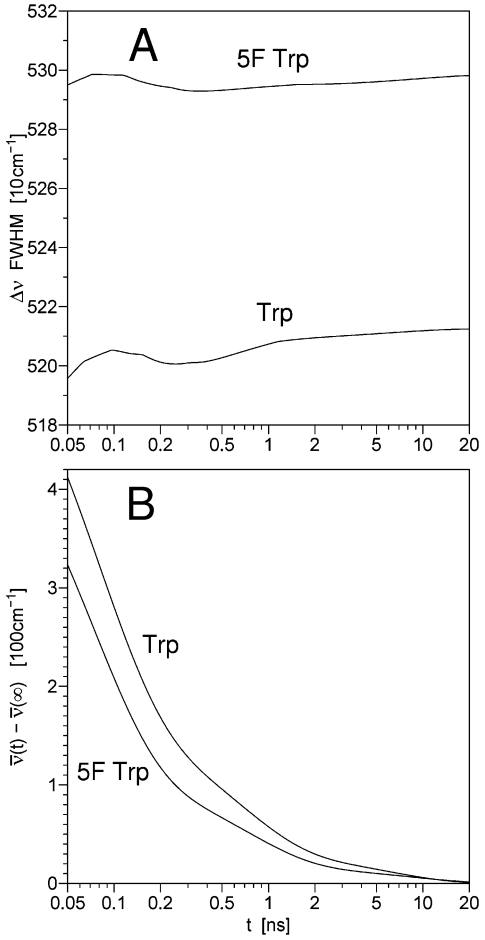

Figure 4. (A) Time variation of the full width at half-maximum of the instantaneous emission spectra shown in Figure 3. (B) Time variation of the centers of gravity $\bar{\nu}$ of the instantaneous emission spectra from Figure 3, with the $t \rightarrow \infty$ limit subtracted. The data for this figure were calculated by using eqs 4, 6, and 7.

with time.[15,22] The presence of static heterogeneity results in the narrowing of the instantaneous emission spectrum at late times after excitation.[15] Instantaneous emission spectra can be easily generated by using the pre-exponential factor spectra $\alpha_n(\nu)$ shown in Figure 2 and the values of the time constants τ_n; spectra generated in this way are devoid of random noise (which is always present in the raw experimental data) and systematic errors, such as photomultiplier background, scattered light, instabilities in the exciting radiation power, etc.

The peak-normalized instantaneous emission spectra generated for 5FTrp and unmodified Trp in GB1 are shown in Figure 3; the spectra exhibit time-invariant spectral widths, consistent with the homogeneous relaxation model.[15,22] The time variation of the full width at half-maximum of the instantaneous emission spectra is displayed in Figure 4A. This figure shows that the emission spectrum of 5FTrp is about 100 cm^{-1} or 2% wider than that of the unmodified Trp. The width varies by 3.5 cm^{-1} or 0.07% and 17.4 cm^{-1} or 0.33% for 5FTrp and unmodified Trp, respectively. These variations are very small and most likely the result of minor systematic errors in the sensitivity curve that was used for spectral correction. The absence of a significant decrease in the width of the instantaneous emission spectra at late times after excitation confirms that we deal with a homogeneous population of excited state fluorophores in relaxing environments rather than with multiple populations in different static environments.[15]

Although the width of the instantaneous emission spectra is virtually time invariant, both the emission peak and the center of gravity shift significantly to the red (to a lower wavenumber) during the first 20 ns after excitation. In Figure 4B we display the time variation of the center of gravity, $\bar{\nu}(t)$; the curves were generated by using eqs 4 and 6. To facilitate the comparison between the $\bar{\nu}(t)$ curves for 5FTrp and Trp, the $t \rightarrow \infty$ limit has been subtracted from each curve. In Figure 35S in the Supporting Information we also show a plot of the two $\bar{\nu}(t)$ curves from which the $t \rightarrow \infty$ limit has not been subtracted. The $\bar{\nu}(\infty)$ values for 5FTrp and Trp are 27 473 and 27 955 cm^{-1}, respectively; these values were calculated with eq 7. The choice of the logarithmic time scales for Figures 4A and 4B allows the inclusion of both the picosecond and the nanosecond dynamics in the same graph. The limits of the time scale are determined at the one end by the time resolution (about 65 ps) and at the other end by the decreasing fluorescence intensity, which makes it difficult to measure the instantaneous emission spectrum after 20 ns.

A comparison of the two curves in Figure 4B demonstrates that the kinetics of the time-dependent red shift is nearly identical for both fluorophores, although the amplitude of the shift is somewhat larger for unmodified Trp (410 cm^{-1}) than for 5FTrp (320 cm^{-1}). Given that the amplitude of the time-

dependent red shift for a solvatochromic fluorophore is proportional to the squared magnitude of the vector difference between its excited state and ground state static electric dipole moment,[37−39] if 5FTrp and the unmodified Trp are in identical environments during the fluorescence measurements, as expected from the invariant structure of 5FTrp-substituted and unsubstituted GB1, the magnitude of the static electric dipole vector change in 5FTrp has to be equal to about 88% of that in the unmodified Trp.

GB1 Relaxation Dynamics. Since the relaxation of bulk water[3] takes only about 1 ps and the relaxation of bound water is not expected to be considerably slower than that,[40] the time-dependent red shift recorded on the time scale between 50 ps and 20 ns undoubtedly represents the relaxation of the protein matrix. Whether the relaxation dynamics is recorded by using Trp or 5FTrp, the $\Delta\bar{\nu}$ versus log(t) curve shown in Figure 4B consists of three linear segments, corresponding to the time windows 50 ps to 200 ps, 200 ps to 2 ns, and 2 ns to 20 ns. The three segments probably correspond to three modes of collective motion with different characteristic times. The greatest slope $-\partial\Delta\bar{\nu}/\partial\ln(t)$ corresponds to the time window 50−200 ps, which represents the fastest and the largest amplitude relaxation mode on the time scale of TCSPC data. This relaxation mode was previously recorded using the fluorescence upconversion technique by other authors, who incorporated the artificial solvatochromic fluorescent amino acid aladan into GB1.[16] Four GB1 mutants were created, in which aladan residues were substituted for the wild type residues L7, A24, F30, and W43, respectively. A significant time-dependent red shift on the time scale 50 to 160 ps was observed only with the W43-aladan mutant.[16] The environment of the fluorophore in this mutant was presumably the same as the environment of the side chains of Trp and 5FTrp in our experiments, and the relaxation dynamics reported in ref 16 is in qualitative agreement with the data shown here. Within the 2 to 20 ns time window the slope $-\partial\Delta\bar{\nu}/\partial\ln(t)$ is close to zero for GB1, in contrast to that of the other proteins studied previously in our laboratory;[15] this points to the fact that the relaxation of GB1 is considerably faster than that of these other proteins.

Frauenfelder and co-workers have extensively studied the dynamics of CO binding to myoglobin in glycerol−water mixtures at cryogenic temperatures; their results support the idea that the relaxation dynamics of the protein follows the stretched exponential model over a broad time scale from microseconds to days.[41−44] It was suggested to us that the same model may also describe the protein dynamics reported by Trp fluorescence on the time scale from picoseconds to nanoseconds. Equation 16 describes the stretched exponential relaxation model in application to the time-dependent red shift in fluorescence emission,

$$\bar{\nu}(t) = \bar{\nu}_\infty + \alpha \exp\{-(kt)^\beta\} \qquad (16)$$

Our common method of global data analysis was not based on fitting eq 16 or any other explicit parametric $\bar{\nu}(t)$ model to experimental data, therefore the results shown in Figures 2−4 cannot help answer the question whether the stretched exponential model adequately describes the time-dependent red shift of Trp in GB1. To answer the latter question we fit the spectrally and time-resolved fluorescence data by a mathematical model obtained by substituting $\bar{\nu}(t)$ from eq 16 into eq 8. Technical details concerning parametrization of the spectral function $S(\nu)$ and the population decay function $N(t)$ are described in the Supporting Information.

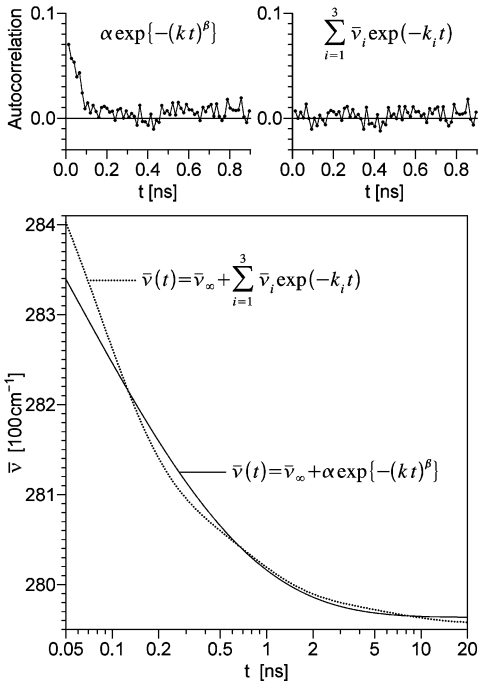

Figure 5. Bottom panel: The $\bar{\nu}(t)$ curves that represent the best fits to the experimental data in the case of the stretched exponential relaxation model (solid line) and the linear combination of three exponentials (dotted line). Top panels: Plots of global autocorrelation of unweighted residuals for the stretched exponential relaxation model (left) and the linear combination of three exponentials (right).

The best fit to the Trp fluorescence data by the stretched exponential relaxation model was achieved with the following values of the fitting parameters: $\bar{\nu}_\infty = 27\,964$ cm^{-1}, $\alpha = 1015$ cm^{-1}, $k = 19.6 \times 10^9$s^{-1}, and $\beta = 0.365$; the corresponding $\bar{\nu}(t)$ curve is shown by the solid line in Figure 5. The reduced χ^2 for the stretched exponential fit equals 1.041, which is outside the range of tolerable χ^2 values (for an adequate fit to the data with 60 000 degrees of freedom, with a probability of 99% the reduced χ^2 value should lie between 0.985 and 1.015). Systematic errors are also revealed by the autocorrelation of residuals (top left panel in Figure 5) and by the global color map of weighted residuals in the Supporting Information (Figure 36S).

The inadequate fit by the stretched exponential relaxation model is most likely due to the insufficient number of fitting parameters: the model has only three fitting parameters, not counting the $\bar{\nu}_\infty$ baseline. A linear combination of two common exponentials (four fitting parameters) also produced an inadequate fit; however, in the case of three common exponentials (six fitting parameters) a statistically adequate fit was achieved with the reduced χ^2 value of 1.005, see also the autocorrelation of residuals (top right panel in Figure 5). The following values of the fitting parameters produced the best fit: $\bar{\nu}_\infty = 27\,957$ cm^{-1}, $\bar{\nu}_1 = 520$ cm^{-1}, $k_1 = 13.0 \times 10^9$ s^{-1}, $\bar{\nu}_2 = 148$ cm^{-1}, $k_2 = 1.57 \times 10^9$s^{-1}, $\bar{\nu}_3 = 38$ cm^{-1}, and $k_3 = 0.18 \times 10^9$s^{-1}; the corresponding $\bar{\nu}(t)$ curve is shown by the dotted line in Figure 5. The solid and the dotted curve cross four times (one crossing at $t = 4.7$ ps is outside the time window of Figure 5). The differences between the solid and the dotted line appear to be small, implying that the stretched exponential relaxation model provides a very close approximation to the real $\bar{\nu}(t)$ curve.

Among the results of Frauenfelder and co-workers, the conclusion that protein relaxation dynamics can be approximated by the stretched exponential model is probably less important than the finding that the rate of protein relaxation varies directly proportional to the rate of solvent relaxation. This phenomenon,

known as slaving,[42−44] was experimentally studied by varying the temperature in 3:1 glycerol−water mixed solvent, producing a many orders of magnitude change in viscosity.[42] Unfortunately, glycerol is an unacceptable cosolvent for Trp fluorescence experiments, because the relaxation of glycerol itself takes place on the nanosecond time scale,[22] and in the presence of glycerol the $\bar{\nu}(t)$ curves are overwhelmed by the solvent relaxation. Varying the temperature of pure water without glycerol does not produce a viscosity change large enough to study its effect on protein dynamics. This explains why we have not attempted to study slaving using the time-dependent red shift in Trp fluorescence. Such a study may be possible if a suitable cosolvent is found, which does not relax on the nanosecond time scale (e.g., acetonitrile).

Decay of the Excited State Fluorophore Population. The time-dependent spectral shift carries important information about the relaxation dynamics in the fluorophore environment. Information of a different kind is contained in the decay of the excited state fluorophore population. The variation of the number N of fluorescent molecules in the excited state with the time t after excitation describes the decay of the excited state population, $N(t)$. For a homogeneous excited state fluorophore population the decay can be calculated by solving for $t > 0$ the differential equation

$$\frac{\partial N(t)}{\partial t} = -k_r(t)N(t) - k_{nr}(t)N(t) \qquad (17)$$

In the case of a nonsolvatochromic fluorophore and/or completely nonpolar environment, the radiative decay rate k_r and the nonradiative decay rate k_{nr} are time-invariant, and therefore the decay of the excited state is described by the monoexponential law. For a solvatochromic fluorophore like Trp or 5FTrp in a protein matrix, microscopic dielectric relaxation of the fluorophore environment results in a time variation of both rates.[45] The behavior of the sum $k_r + k_{nr}$ can be calculated by using eq 18, which has been obtained by swapping the right-hand side with the left-hand side of eq 17 and dividing both sides by $-N(t)$

$$k_r(t) + k_{nr}(t) = -\frac{\partial \ln[N(t)]}{\partial t} \qquad (18)$$

The right-hand side of eq 18 can be calculated from the spectrally and time-resolved fluorescence intensity $F_\nu(\nu,t)$ by using eq 13 or directly form the fitting parameters obtained in the course of the global fitting by using eqs 6 and 15; the latter method was used to generate the $k_r + k_{nr}$ versus $\log(t)$ curves depicted in Figure 6.

Figure 6 shows that during the time window between 50 ps and 20 ns, the sum $k_r + k_{nr}$ decreases from about 22.5×10^7 to about 18×10^7 s^{-1} (1.25-fold) in the case of 5FTrp and from about 24.5×10^7 to about 14×10^7 s^{-1} (1.75-fold) in the case of unmodified Trp. Since the radiative decay rate is directly proportional to the mean cube of the emission frequency,[46] it is not difficult to estimate the magnitude of the variation in k_r. For the Trp residue in GB1, the radiative decay rate decreases only 1.045-fold, which is clearly insufficient to explain the 1.75-fold change in the sum $k_r + k_{nr}$. For 5FTrp in GB1, k_r decreases only 1.036-fold, which is insufficient to explain the 1.25-fold change in the sum $k_r + k_{nr}$. This shows that the changes in the sum $k_r + k_{nr}$ are caused primarily by the changes in k_{nr}. Indeed, the rates for some nonradiative decay mechanisms are expected to vary significantly during the time-dependent red shift. For example, electron transfer from an excited state Trp residue to the protein backbone requires that the energy of the electron-transfer state is lower than that of the excited state Trp residue.[25] The energy of the excited state Trp residue decreases by some 410 cm^{-1} during the 50 ps to 20 ns time window (see Figure 4B); this may be sufficient to slow the electron transfer dramatically and may result in a several-fold variation in k_{nr}. For 5FTrp the initial energy of the excited state at early times after excitation is some 570 cm^{-1} lower than that for the unmodified Trp, therefore the rate of electron transfer from 5FTrp to the backbone is lower and the amplitude of k_{nr} variation is smaller than in the case of Trp.

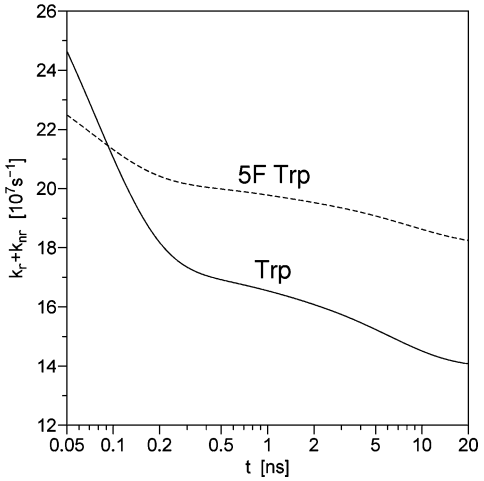

Figure 6. Time variation of the sum of the radiative and nonradiative decay rates, calculated as $-\partial \ln[N(t)]/\partial t$, using eqs 6 and 15.

The decrease in the energy of the excited state renders the excited fluorophore chemically less reactive, which means that the rate of any excited state reaction decreases during the course of solvent and protein relaxation. Every excited state reaction depopulates (quenches) the excited state, and since k_{nr} equals the sum of the rates for all quenching mechanisms, it is expected to vary with time if the rate of at least one excited state reaction is time dependent. Excited state proton transfer from a proton donor (such as an amino group) to the fourth[47,48] or seventh[47] ring carbon of the Trp side chain can also contribute to the time variation of k_{nr}. The rate of proton transfer is likely to be affected by the fluoride substitution on the fifth carbon, which explains the differences in the time-resolved fluorescence between unmodified Trp and 5FTrp. Thus, not only electron transfer to the protein backbone,[25] but also proton transfer to the Trp side chain[47,48] may be responsible for the larger amplitude of $k_r + k_{nr}$ variation in the case of unmodified Trp compared to a smaller amplitude in the case of 5FTrp. An experimental approach for decreasing the proton-transfer quenching rate is based on $H_2O \rightarrow D_2O$ solvent replacement;[47] thus, it should be possible to differentiate between electron transfer and proton transfer by using this approach.

Irrespective of whether electron transfer or proton transfer is the dominant quenching mechanism, the energy dependence of k_{nr} in combination with the time-dependent excited state energy results in a decay law that differs from the monoexponential model, with this difference expected to be larger for Trp than for 5FTrp. In accord with this prediction, the deviation of the excited fluorophore population decay in GB1 from the monoexponential decay law is significantly larger in the case of Trp than in the case of 5FTrp, see Figure 6. The data obtained by Broos and co-workers[24] as well as Winkler and co-workers[34] point to the fact that in several other proteins the decay of Trp deviates from the monoexponential law more significantly than

that of 5FTrp; however, they interpret this result in terms of static heterogeneity[24,25,34] rather than in terms of the time variation of the nonradiative decay rate. In the case of GB1 the conservation of the shape (Figure 3) and width (Figure 4A) of the time-resolved emission spectra is inconsistent with the presence of static heterogeneity, therefore the time variation of k_{nr} is the only mechanism that can explain the deviations from the monoexponential decay law for Trp and 5FTrp in this protein. For the proteins studied in refs 24 and 34 no time-resolved emission spectra are available, therefore both static heterogeneity and the time variation of the nonradiative decay rate may contribute to the deviations from the monoexponential decay law for those proteins.

Static heterogeneity is expected in a protein containing more than one Trp residue in its aminoacid sequence, since every Trp residue retains its individual environment forever.[30] A protein with a single Trp residue can also exhibit a heterogeneous fluorescence signal, if multiple conformations of the local Trp environment exist, and the interconversion between these conformations is much slower than the decay of the excited state. Thermal motion of protein atoms (including the rotation of the Trp side chain about the χ_1 and χ_2 axes) results in an infinite variety of different conformations of the Trp environment, but this can produce a heterogeneous fluorescence signal only if the characteristic interconversion time exceeds the excited state lifetime. The time it takes to switch from one protein conformation to another depends on the protein size and structural integrity, as well as the solvent viscosity and temperature. Interconversion times greater than 10 ns are expected for large proteins (>50 kD), unfolded, partially unfolded, naturally unfolded, or denatured proteins, aggregated proteins, proteins with extensive naturally disordered regions, proteins in high-viscosity solvents, detergent micelles, or lipid membranes, and proteins frozen in low-temperature glasses. A 68 kD integral membrane protein in detergent micelles is likely to have interconversion times much longer than 10 ns, and therefore static heterogeneity can easily play a role in the decay of fluorescence emission from the single-Trp IIA^{mtl} mutants studied by Broos and co-workers.[24,25] It must be emphasized that for proteins with heterogeneous Trp fluorescence signals, $\bar{\nu}(t)$ curves do not represent relaxation dynamics, and therefore protein dynamics studies utilizing the time-dependent red shift should be limited to small water-soluble thermodynamically stable single-Trp proteins of high structural integrity, of which GB1 is a perfect example.

Conclusion

Spectrally and time-resolved fluorescence emission from Trp or 5FTrp in GB1 exhibits no indication of static heterogeneity (which would result in the narrowing of the instantaneous emission spectrum at long times after excitation), but clearly shows a time-dependent red shift, characteristic of microscopic dielectric relaxation. The lack of static heterogeneity is consistent with GB1 having a single equilibrium conformation under our measurement conditions (subnanosecond fluctuations produce no static heterogeneity).

It is remarkable that the relaxation dynamics reported by the time-dependent red shifts in the fluorescence of 5FTrp and unmodified Trp are essentially identical. This confirms that the recorded red shift is a characteristic of the protein matrix rather than of the fluorophore itself. The total amplitude (but not the rate) of the time-dependent red shift is affected by a fluorophore property, namely, the magnitude of the vector difference between the excited state and ground state electric dipole moment. On the basis of the experimental data, for 5FTrp this magnitude is estimated to be about 88% of that for unmodified Trp.

The decay of the excited state fluorophore population is not monoexponential for both Trp and 5FTrp in GB1; however, the deviation from the monoexponential decay law is considerably larger in the case of unmodified Trp. The non-monoexponential decays are interpreted in terms of the energy-dependent rates of some quenching mechanisms, which include electron transfer and proton transfer.

The relaxation dynamics of GB1 appears to be considerably faster than that of other proteins we studied previously in our laboratory.[15] This exceptionally fast relaxation dynamics is probably a result of the combination of the small size, tightly packed core, and high thermodynamic stability of GB1.

Acknowledgment. The authors thank Dr. Jaap Broos, Dr. Patrik R. Callis, and Dr. Jay R. Knutson for interesting discussions of our preliminary results and suggestions regarding their possible explanations. D.T. and L.B. also thank Dr. Blake Hill and Dr. Guru Thuduppathy for bringing GB1 to our attention. This work was supported by the National Science Foundation award MCB-0416965 and the Intramural Research Program of the NIH, NIDDK (A.M.G.).

Supporting Information Available: A schematic diagram and a typical impulse response function of the experimental setup for spectrally resolved time-correlated photon counting; plots of the data with fit, weighted residuals and autocorrelation of the residuals for six selected emission wavelengths (325, 355, and 390 nm for 5FTrp and 320, 350, and 385 nm for the unmodified Trp) and for five multiexponential model functions ($N_{exp} = 1, 2, 3, 4, 5$); values of the parameters α_n and τ_n for the model with the smallest N_{exp} that produced a statistically adequate fit at each of the six emission wavelengths; fluorescence kinetics of 5FTrp and Trp in GB1, presented in the format of Figure 1 in ref 24; a figure similar to Figure 4B, where the absolute $\bar{\nu}(t)$ data are shown (without the $t \rightarrow \infty$ limit subtracted); technical details concerning parametrization of the spectral function $S(\nu)$ and the population decay function $N(t)$ when fitting the spectrally and time-resolved fluorescence data by a model based on eq 8; and color maps of weighted residuals for the stretched exponential relaxation model and the linear combination of three common exponentials. This material is available free of charge via the Internet at http://pubs.acs.org.

References and Notes

(1) The time-dependent red shift is also known as the fluorescence dynamic Stokes shift. Time-resolved fluorescence spectroscopy as well as pump-probe transient gain/absorption spectroscopy and three-pulse photon echo techniques can be used to gain information about microscopic dielectric relaxation in the environment of a solvatochromic fluorophore.

(2) Maroncelli, M. *J. Mol. Liq.* **1993**, *57*, 1−37.

(3) Jimenez, R.; Fleming, G. R.; Kumar, P. V.; Maroncelli, M. *Nature* **1994**, *369*, 471−473.

(4) Horng, M. L.; Gardecki, J. A.; Papazyan, A.; Maroncelli, M. *J. Phys. Chem.* **1995**, *99*, 17311−17337.

(5) Stratt, R. M.; Maroncelli, M. *J. Phys. Chem.* **1996**, *100*, 12981−12996.

(6) Brand, L.; Gohlke, J. R. *J. Biol. Chem.* **1971**, *246*, 2317−2319.

(7) Gafni, A.; DeToma, R. P.; Manrow, R. E.; Brand, L. *Biophys. J.* **1977**, *17*, 155−168.

(8) Lakowicz, J. R.; Gratton, E.; Cherek, H.; Maliwal, B. P.; Laczko, G. *J. Biol. Chem.* **1984**, *259*, 10967−10972.

(9) Pierce, D. W.; Boxer, S. G. *J. Phys. Chem.* **1992**, *96*, 5560−5566.

(10) Wang, R.; Sun, S.; Bekos, E. J.; Bright, F. V. *Anal. Chem.* **1995**, *67*, 149−159.

(11) Lundgren, J. S.; Bright, F. V. *J. Phys. Chem.* **1996**, *100*, 8580−8586.

(12) Riter, R. R.; Edington, M. D.; Beck, W. F. *J. Phys. Chem.* **1996**, *100*, 14198−14205.
(13) Jordanides, X. J.; Lang, M. J.; Song, X.; Fleming, G. R. *J. Phys. Chem. B* **1999**, *103*, 7995−8005.
(14) Vincent, M.; Gilles, A.-M.; de la Sierra, I. M. L.; Briozzo, P.; Barzu, O.; Gallay, J. *J. Chem. Phys. B* **2000**, *104*, 11286−11295.
(15) Toptygin, D.; Savtchenko, R. S.; Meadow, N. D.; Brand, L. *J. Phys. Chem. B* **2001**, *105*, 2043−2055.
(16) Cohen, B. E.; McAnaney, T. B.; Park, E. S.; Jan, Y. N.; Boxer, S. G.; Jan, L. Y. *Science* **2002**, *296*, 1700−1703.
(17) Sen, P.; Mukherjee, S.; Dutta, P.; Halder, A.; Mandal, D.; Banerjee, R.; Roy, S.; Bhattacharyya, K. *J. Phys. Chem. B* **2003**, *107*, 14563−14568.
(18) Lampa-Pastirk, S; Beck, W. F. *J. Phys. Chem. B* **2004**, *108*, 16288−16294.
(19) Hutterer, R.; Schneider, F. W.; Lanig, H.; Hof, M. *Biochim. Biophys. Acta* **1997**, *1323*, 195−207.
(20) Somoza, M. M.; Andreatta, D.; Murphy, C. J.; Coleman, R. S.; Berg, M. A. *Nucleic Acids Res.* **2004**, *32*, 2494−2507.
(21) The term monoexponential is used throughout this paper to describe a fluorescence kinetic curve or a decay curve $f(t)$ that equals zero before δ-excitation at $t = 0$ and equals $\alpha \exp(-t/\tau)$ at $t > 0$, i.e., $f(t) = \alpha\theta(t) \exp(-t/\tau)$, where $\theta(t)$ denotes the Heaviside step function. The terms non-monoexponential and multiexponential are both antonyms of monoexponential, although in theory they have different meanings. Since any fluorescence kinetic curve can be adequately represented by a linear combination of a finite number of exponential terms (the number of required terms depending on the data quality), from the practical point of view any non-monoexponential curve is also a multiexponential curve and vise versa.
(22) Toptygin, D.; Brand, L. *Chem. Phys. Lett.* **2000**, *322*, 496−502.
(23) Peticolas, W. L. *Methods Enzymol.* **1979**, *61*, 425−458.
(24) Broos, J.; Maddalena, F.; Hesp, B. H. *J. Am. Chem. Soc.* **2004**, *126*, 22−23.
(25) Liu, T.; Callis, P. R.; Hesp, B. H.; de Groot, M.; Buma, W. J.; Broos, J. *J. Am. Chem. Soc.* **2005**, *127*, 4104−4113.
(26) Gronenborn, A. M.; Filpula, D. R.; Essing, N. Z.; Achari, A.; Whitlow, M.; Wingfield, P. T.; Clore, M. G. *Science* **1991**, *253*, 657−661.
(27) Kuszewski, J.; Gronenborn, A. M.; Clore, G. M. *J. Am. Chem. Soc.* **1999**, *121*, 2337−2338.
(28) Gallagher, T.; Alexander, P.; Bryan, P.; Gilliland, G. L. *Biochemistry* **1994**, *33*, 4721−4729.
(29) Toptygin, D.; Rodgers, M. E.; Brand, L. *Biophys. J.* **1999**, *76*, A361.
(30) Ross, J. B. A.; Schmidt, C. J.; Brand, L. *Biochemistry* **1981**, *20*, 4369−4377.
(31) Hirshfield, K. M.; Toptygin, D.; Grandhige, G.; Packard, B. Z.; Brand, L. *Biophys. Chem.* **1998**, *71*, 63−72.
(32) The number of degrees of freedom equals the number of channels where photon counts are stored minus the number of fitting parameters. For global fitting the number of channels per kinetic curve must be multiplied by the number of kinetic curves; this product less the total number of all (global + local) fitting parameters equals the number of degrees of freedom.
(33) Hamilton, W. C. *Statistics in Physical Science*; Ronald Press Co.: New York, 1964.
(34) Winkler, G. R.; Harkins, S. B.; Lee, J. C.; Gray, H. B. *J. Phys. Chem. B* **2006**, *110*, 7058−7061.
(35) Gafni, A.; Brand, L. *Biochemistry* **1976**, *15*, 3165−3171.
(36) Tcherkasskaya, O.; Knutson, J. R.; Bowley, S. A.; Frank, M. K.; Gronenborn, A. M. *Biochemistry* **2000**, *39*, 11216−11226.
(37) Mataga, N.; Kaifu, Y.; Koizumi, M. *Bull. Chem. Soc. Jpn.* **1955**, *28*, 690−691.
(38) Mataga, N.; Kaifu, Y.; Koizumi, M. *Bull. Chem. Soc. Jpn.* **1956**, *29*, 465−470.
(39) McRae, E. G. *J. Phys. Chem.* **1957**, *61*, 562−572.
(40) Nilsson, L.; Halle, B. *Proc. Natl. Acad. Sci. U.S.A.* **2005**, *102*, 13867−13872.
(41) Frauenfelder, H.; Sligar, S. G.; Wolynes, P. G. *Science* **1991**, *254*, 1598−1603.
(42) Fenimore, P. W.; Frauenfelder, H.; McMahon, B. H.; Parak, F. G. *Proc. Natl. Acad. Sci. U.S.A.* **2002**, *99*, 16047−16051.
(43) Fenimore, P. W.; Frauenfelder, H.; McMahon, B. H.; Young, R. D. *Physica A* **2005**, *351*, 1−13.
(44) Lubchenko, V.; Wolynes, P. G.; Frauenfelder, H. *J. Phys. Chem. B* **2005**, *109*, 7488−7499.
(45) Mei, G.; Di Venere, A.; Agro, A. F.; De Matteis, F.; Rosato, N. *J. Fluoresc.* **2003**, *13*, 467−477.
(46) Toptygin, D.; Savtchenko, R. S.; Meadow, N. D.; Roseman, S.; Brand, L. *J. Phys. Chem. B* **2002**, *106*, 3724−3734.
(47) Yu, H. T.; Colucci, W. J.; McLaughlin M. L.; Barkley, M. D. *J. Am. Chem. Soc.* **1992**, *114*, 8449−8454.
(48) Blankafort, L.; Gonzalez, D.; Olivucci, M.; Robb, M. A. *J. Am. Chem. Soc.* **2002**, *124*, 6398−6406.